Journal of Computational Neuroscience
https://doi.org/10.1007/s10827-017-0674-4

Coding of time-dependent stimuli in homogeneous and heterogeneous neural populations

Manuel Beiran[1,4] · **Alexandra Kruscha**[1,2] · **Jan Benda**[3] · **Benjamin Lindner**[1,2]

Received: 28 June 2017 / Revised: 8 November 2017 / Accepted: 12 November 2017

Abstract

We compare the information transmission of a time-dependent signal by two types of uncoupled neuron populations that differ in their sources of variability: i) a *homogeneous population* whose units receive independent noise and ii) a deterministic *heterogeneous population*, where each unit exhibits a different baseline firing rate ('disorder'). Our criterion for making both sources of variability quantitatively comparable is that the interspike-interval distributions are identical for both systems. Numerical simulations using leaky integrate-and-fire neurons unveil that a non-zero amount of both noise or disorder maximizes the encoding efficiency of the homogeneous and heterogeneous system, respectively, as a particular case of suprathreshold stochastic resonance. Our findings thus illustrate that heterogeneity can render similarly profitable effects for neuronal populations as dynamic noise. The optimal noise/disorder depends on the system size and the properties of the stimulus such as its intensity or cutoff frequency. We find that weak stimuli are better encoded by a noiseless heterogeneous population, whereas for strong stimuli a homogeneous population outperforms an equivalent heterogeneous system up to a moderate noise level. Furthermore, we derive analytical expressions of the coherence function for the cases of very strong noise and of vanishing intrinsic noise or heterogeneity, which predict the existence of an optimal noise intensity. Our results show that, depending on the type of signal, noise as well as heterogeneity can enhance the encoding performance of neuronal populations.

Keywords Integrate-and-fire neuron · Noise · Heterogeneity · Stochastic resonance · Population coding

1 Introduction

The ability of the nervous system to reliably process information from the outer environment is essential for the survival and reproduction of an organism. However, the *in vivo* response of neurons to a repeated stimulus is usually highly variable. Furthermore, neurons that belong to the same neural structures show a wide diversity of excitability properties. Two types of variability are observed: (i) unreliability of responses at the single neuron level caused by intrinsic neural noise and (ii) heterogeneity at the population level. Both of them influence notably the information transmission properties of neural populations. The sources of variability, such as channel noise (Fox 1997; Steinmetz et al. 2000; Schmid et al. 2004; Fisch et al. 2012) and background synaptic input (e.g. Shadlen and Newsome (1994), van Vreeswijk and Sompolinsky (1996), Brunel (2000), and Dummer et al. (2014)) and their effects on information transmission (Chance et al. 2002; Chacron et al. 2003; Wolfart et al. 2005; Vilela and Lindner 2009b; Sceniak and Sabo 2010) have been extensively studied in the last decades, while the effects of neural heterogeneity have come into focus only more recently (Chelaru and Dragoi 2008; Osborne et al. 2008; Homstron et al. 2010; Marsat and Maler 2010; Mejias and Longtin 2014; Metzen and Chacron 2015).

Intrinsic neural noise can be understood as the dynamic stochastic variations in the membrane voltage of neurons or

Action Editor: Brent Doiron

✉ Manuel Beiran
manuel.beiran@ens.fr

[1] Bernstein Center for Computational Neuroscience Berlin, Berlin, Germany

[2] Physics Department, Humboldt-Universität zu Berlin, Berlin, Germany

[3] Institute for Neurobiology, Eberhard Karls Universität, Tübingen, Germany

[4] Present address: Group for Neural Theory, Laboratoire de Neurosciences Cognitives, Département Études Cognitives, École Normale Supérieure, INSERM, PSL Research University, Paris, France

Published online: 08 December 2017

as the source of these variations, e.g. channel fluctuations or random synaptic input from other neurons. Theoretical work has shown that noise in nonlinear systems is not necessarily detrimental for signal encoding, one example of which is the well-known stochastic resonance (SR) effect (Gammaitoni et al. 1998; McDonnell and Ward 2011). SR refers to the enhancement of the response to a weak signal by a nonlinear system when a non-zero amount of intrinsic noise is present. SR was first proposed in the early 1980s in climate research (Benzi et al. 1981; Nicolis 1982) and has been found in nonlinear systems of different fields including single neurons (Longtin 1993; Wiesenfeld and Moss 1995; McDonnell and Ward 2011). A particular case of SR that applies to systems of multiple parallel nonlinear units was discovered by Stocks (2000): the stochastic suprathreshold resonance (SSR) effect. This is a general phenomenon found in nonlinear systems of several feed-forward parallel units that receive the same input stimulus; SSR has been studied more recently in a number of systems (Stocks and Mannella 2001; Das et al. 2009; Ashida and Kubo 2010; Durrant et al. 2011). A certain non-zero amount of independent noise on each unit can improve the transmission of the signal by the system, but in contrast to classical SR, the SSR effect applies as well to the cases of strong input signals or suprathreshold systems, i.e. structures formed by units that emit a response even if no signal or noise is present. It has been observed in various neural systems such as multilevel threshold units (Stocks 2000), populations of non-interacting FitzHugh-Nagumo (FHN), leaky integrate-and fire (LIF) or Hodgkin-Huxley model neurons (Stocks and Mannella 2001; Hoch et al. 2003; Nikitin et al. 2010; Hunsberger et al. 2014).

Neuronal heterogeneity, understood as some type of parametric variability within a certain population of neurons, is neglected in many biophysical network models, yet it is ubiquitous in the nervous system (for a recent experimental study of neural heterogeneity, see Harrison et al. (2015)). The most intensely studied aspect regarding heterogeneity is the large differences between the firing rates of neurons of the same population. This variability of the firing rates has been found to be long-tailed and non-Gaussian distributed for neural populations in sensory neurons (Gussin et al. 2007) and several cortical structures (Shafi et al. 2007; Hromádka et al. 2008; O'Connor et al. 2010). However, the general effects of this heterogeneity are difficult to determine from a theoretical point of view, and, in particular, the comparison of dynamical noise and static disorder is not easily feasible.

Several theoretical studies have addressed specific features related to heterogeneity in the last decade. Already in the first work on SSR (Stocks 2000), the threshold variability in independent parallel devices was analytically studied as a way of optimizing the information transmission. Regarding neural coding, heterogeneous populations generally increase the encoded information (Padmanabhan and Urban 2010; Shamir and Sompolinsky 2006), which is optimized at finite levels of heterogeneity (Mejias and Longtin 2012; Tripathy et al. 2013). In particular, heterogeneity, which is sometimes also denoted as frozen or quenched disorder, has been studied in models of cortical networks with special focus on its implications on synchronization (Golomb and Rinzel 1993; Ostojic et al. 2009b; Olmi et al. 2010). More recently, Hunsberger et al. (2014) compared the benefits of noise and heterogeneity on neural coding by including both variability sources simultaneously on populations of FHN and LIF neurons.

The goal of our study is to compare in a systematic way the information processing of a time-dependent signal by two simple neural populations of uncoupled neurons: a homogeneous population whose units receive independent noise and a heterogeneous population of deterministic neurons (a system with static disorder); Alijani and Richardson (2011) make use of two similar systems as limit cases to study analytically the rate response of exponential integrate-and-fire neurons. As an essential novelty in our study, we present a criterion in the design of the two systems, namely the statistical distribution of the interspike intervals, that allows to compare quantitatively the signal-response behavior of both homogeneous and heterogeneous populations. This approach is similar in spirit to the comparison of different neuron models, which are constraint by their firing rate and spiking variability (Vilela and Lindner 2009a, b).

Although the comparatively simple case of uncoupled neurons studied here may look rather restrictive, it includes important examples for neural populations in the sensory periphery, e.g. vertebrate and invertebrate auditory afferents, vestibular afferents, olfactory afferents and electroreceptor afferents. These receptor populations vary considerably in their reliability and heterogeneity (e.g. vestibular: Sadeghi et al. (2007), electroreceptors: Grewe et al. (2017)). Moreover, the comparison between the effects of intrinsic noise and heterogeneity is much simpler than it would be in a recurrent network, in which the strongest source of variability are the input currents from many other cells. Our results thus provide insights about fundamental features of population coding in the sensory periphery.

2 Model and measures of interest

We consider two populations of N uncoupled leaky integrate-and-fire (LIF) neurons receiving a common stimulus $s(t)$. The voltage dynamics of each neuron i is given by

$$\dot{v}_i = -v_i + \mu_i + \sqrt{2D_i}\,\xi_i(t) + s(t), \tag{1}$$

where μ_i and D_i are the mean and noise intensity of the input current intrinsic to the neuron. Noise sources are correlated as $\langle \xi_i(t)\xi_j(t')\rangle = \delta_{ij}\delta(t-t')$. When the voltage variable $v_i(t)$ crosses the threshold v_T, a spike is emitted, the voltage variable is kept at the reset voltage v_R for a refractory period τ_{ref} and released from this value afterwards. The stimulus $s(t)$ is the same for all neurons in both populations and is defined as a band-limited Gaussian process with standard deviation σ_s and cutoff frequency f_c. The spike train of each neuron is given by a sum of delta-functions $x_i(t) = \sum_k \delta(t - t_{i,k})$, where $t_{i,k}$ corresponds to the time of the k-th spike of neuron i. Unless specified otherwise, the following parameter values are fixed for all simulations : $v_T = 1$, $v_R = 0$, $\tau_{ref} = 0.1$.

A useful approach to characterize the neural firing is to study the statistics of the interspike interval (ISI), which are the time differences between two subsequent spike times, $T_k = t_{i,k} - t_{i,k-1}$. The ISI probability density of a LIF neuron, $\rho_{LIF}(T;\mu,D)$, is equivalent to the first passage time distribution of an Ornstein-Uhlenbeck process (OUP) with an absorbing barrier, and can be analytically expressed in the Fourier domain as (Darling and Siegert 1953)

$$\widetilde{\rho}_{LIF}(f;\mu,D) = e^{\Delta + i2\pi f\tau_{ref}} \frac{\mathcal{D}_{i2\pi f}\left(\frac{\mu - v_R}{\sqrt{D}}\right)}{\mathcal{D}_{i2\pi f}\left(\frac{\mu - v_T}{\sqrt{D}}\right)}, \qquad (2)$$

$$\Delta := \frac{v_R^2 + v_T^2 + 2\mu_i(v_T - v_R)}{4D},$$

where $\mathcal{D}_a(b)$ is the parabolic cylinder function.

The homogeneous population consists of statistically equivalent neurons, i.e. the mean input curent and noise intensity to all neurons are the same: $\mu_i^{hom} = \mu_{hom}$ and $D_i^{hom} = D_{hom}$ for $i = 1,\ldots,N$. On the contrary, neurons of the heterogeneous population are not subject to any intrinsic noise, $D_i^{het} = 0$, and each neuron receives a different mean input current, $\mu_i^{het} = \mu_i$, which is sampled from a certain probability density $P(\mu)$. Note that for every trial of the signal, we resample the N values of μ and thus we deal with a system that slowly changes its parameters (comparable to the situation addressed by Alijani and Richardson (2011)) rather than a system in which the N input currents, μ_i, are fixed for all times and, in particular, across trials.

In the following, the population size is assumed to be large enough ($N \gg 1$) so that deviations between the probability density $P(\mu)$ and the distribution of the N samples are small. We will not use, however, excessively large values of N because our setup with the common time-dependent stimulus implies that we deal with a subpopulation of neurons with strongly overlapping receptive fields. As a standard value, we use $N = 300$ (see e.g. Maler (2009) for typical numbers in an electrosensory system).

The goal of this study is to analyze how much information of the common stimulus is contained in the population output. For simplicity, the output function considered is the (unfiltered) population activity,

$$x(t) = \frac{1}{N}\sum_{i=1}^{N} x_i(t)\,. \qquad (3)$$

In order to quantify information transmission, it is relevant to introduce the output power spectrum and the input-output cross-spectrum. Given the output function $x(t)$ and the input stimulus $s(t)$, they are defined as

$$S_{xx}(f) = \lim_{T_W\to\infty} \frac{\langle \tilde{x}^*(f)\tilde{x}(f)\rangle}{T_W} \quad \text{and}$$

$$S_{xs}(f) = \lim_{T_W\to\infty} \frac{\langle \tilde{x}^*(f)\tilde{s}(f)\rangle}{T_W}, \qquad (4)$$

where $\tilde{x}(f) = \int_0^{T_W} e^{i2\pi ft}x(t)dt$ is the Fourier transform over a time window of length T_W, the asterisk indicates the complex conjugate and the angle brackets denote the average over trials and stimuli. The power spectrum of the band-limited Gaussian signal is flat by construction and different from zero only up to the cutoff frequency: $S_{ss} = \frac{\sigma_s^2}{2f_c}\Theta(f_c - |f|)$. The output power spectrum of a single LIF neuron can be expressed analytically as (Lindner et al. 2002)

$$S_{x_i x_i}^{\mathrm{LIF}}(f;\mu,D,\tau_{ref}) = \frac{1}{\langle T\rangle_{\mu,D}} \cdot \frac{\left|\mathcal{D}_{i2\pi f}\left(\frac{\mu-v_T}{\sqrt{D}}\right)\right|^2 - e^{2\Delta}\left|\mathcal{D}_{i2\pi f}\left(\frac{\mu-v_R}{\sqrt{D}}\right)\right|^2}{\left|\mathcal{D}_{i2\pi f}\left(\frac{\mu-v_T}{\sqrt{D}}\right) - e^{\Delta}e^{i2\pi f\tau_{ref}}\mathcal{D}_{i2\pi f}\left(\frac{\mu-v_R}{\sqrt{D}}\right)\right|^2}, \qquad (5)$$

for frequencies $f > 0$.

The input-output cross-spectrum of a single neuron cannot be determined analytically in the general case. However, it can be approximated applying linear response theory assuming that the stimulus is weak compared to the intrinsic noise. In that regime, the average response function of neuron i is described as the convolution of the input signal with a linear filter, which is expressed in the Fourier domain as

$$\langle \tilde{x}_i(f)\rangle = \chi\left(f;\mu,D,\tau_{ref}\right)\tilde{s}(f;\sigma_s,f_c); \qquad f > 0. \qquad (6)$$

A closed analytical form of the Fourier transform of the linear response kernel (the susceptibility χ) exists for LIF neurons (Brunel et al. 2001; Lindner and Schimansky-Geier 2001). It reads

$$\chi_{LIF}\left(f;\mu,D,\tau_{ref}\right)=\frac{1}{\langle T\rangle_{\mu,D}}\cdot\frac{2\pi if/\sqrt{D}}{2\pi if-1}\cdot\frac{\mathcal{D}_{2\pi if-1}\left(\frac{\mu-v_T}{\sqrt{D}}\right)-e^{\Delta}\mathcal{D}_{2\pi if-1}\left(\frac{\mu-v_R}{\sqrt{D}}\right)}{\mathcal{D}_{2\pi if-1}\left(\frac{\mu-v_T}{\sqrt{D}}\right)-e^{\Delta}\mathcal{D}_{2\pi if}\left(\frac{\mu-v_R}{\sqrt{D}}\right)}. \tag{7}$$

Making use of these spectral measures, the input-output correlation can be quantified in a frequency-resolved manner by the spectral coherence function

$$C\left(f\right)=\frac{\left|S_{xs}\left(f\right)\right|^2}{S_{xx}(f)S_{ss}(f)}, \tag{8}$$

which can attain values between zero (no linear correlation whatsoever) and one (perfect linear and noiseless signal transmission) for a given frequency component of the stimulus and the output. Finally, based on these spectral statistics, the efficiency of information transfer of a certain system is assessed in this study by the coding fraction γ. The coding fraction is a normalized measure of the quality of the optimal linear reconstruction of the stimulus from the output signal (Gabbiani et al. 1996)

$$\gamma=1-\sqrt{\frac{\epsilon^2}{\sigma^2}}=1-\sqrt{\frac{\int df S_{ss}\left(f\right)\left(1-C\left(f\right)\right)}{\int df S_{ss}\left(f\right)}}, \tag{9}$$

where ϵ^2 is the mean squared error between stimulus and linear reconstruction (Wessel et al. 1996), and σ^2 is the variance of the input. Thus, the coding fraction is zero when the optimal reconstruction performance is at chance level and one for a potentially perfect reconstruction.

Previous studies (Hunsberger et al. 2014; Stocks and Mannella 2001) quantified the encoding efficiency of dynamic stimuli by the mutual information between the response and the signal at a fixed time, thereby ignoring possible delayed responses that also encode information about the signal. In addition, in order to derive the necessary (joint) probability densities of the input and output processes, the signal and response were quite broadly binned making them effectively discrete processes with few possible states. These preprocessing steps to calculate the computationally more costly mutual information delete information content and bias the estimation (Strong et al. 1998). The coding fraction, although only sensitive to linear correlations between input and output, eludes the problem by taking into account all delays of the response and does not require any discretization. Therefore, it constitutes an unambiguous measure of the transmission performance, that can be universally applied to time-dependent input signals.

3 How to compare different kinds of variability

Population encoding of time-dependent stimuli is the process of conveying information about a time-dependent signal to a set of spike trains. A decisive aspect of this process is the number of spikes available to store the information of the stimulus per unit of time in a certain population. Accordingly, we force the number of available spikes per unit of time to be the same in both populations when there is no stimulus present. Moreover, we constrain this criterion even further so that not only the population's mean interspike interval needs to have the same value, but also the whole ISI distributions of both systems must be equal. In other words, we set the ISI density of both populations in the absence of stimulation to be equal in order to compare them.

The ISI density $\rho(T)$ of a neural population is here understood as the probability density function of a random interspike interval to take on a certain value across the whole pool of intervals and neurons of the population. The criterion we set in order to make the homogeneous and the heterogeneous populations comparable then reads

$$\rho_{hom}\left(T;D_{hom},\mu_{hom}\right)\overset{!}{=}\rho_{het}\left(T;P\left(\mu\right)\right), \tag{10}$$

where $\rho(T)$ is the probability density of the interspike intervals T of a certain neural population and all the parametric dependencies are explicitly specified.

Neurons of the homogeneous population are indistinguishable from each other by definition, which makes the ISI density of the homogeneous population identical to the one of any single neuron of the population, $\rho_{hom}\left(T\right)=\rho_{LIF}\left(T\right)$. The ISI density of a single neuron $\rho_{LIF}\left(T\right)$ is obtained by computing the inverse Fourier transform of Eq. (2).

For the heterogeneous system, the ISI density of the population $\rho_{het}(T)$ is the average of the ISI densities of the single neurons weighted by their corresponding firing rate

$$\rho_{het}\left(T,P\left(\mu\right)\right)=\frac{\int d\mu\, P\left(\mu\right)T_{\mu}^{-1}\rho_{LIF}\left(T;\mu,D=0\right)}{\int d\mu'\, P\left(\mu'\right)\cdot T_{\mu'}^{-1}}, \tag{11}$$

where T_μ^{-1} is the firing rate of a noiseless LIF neuron with mean input current μ. The weighted average is necessary to obtain the same number of spikes per unit of time in both populations, avoiding the over-representation of interspike intervals coming from neurons with stronger input current and the underrepresentation of long interspike intervals by neurons with weaker inputs (known as the biased-sampling problem in the statistical literature, see e.g. the textbook by Cox and Lewis (1966)).

The interspike interval of the noiseless LIF neuron is obtained as the (deterministic) passage time from reset voltage to threshold voltage

$$T_\mu = \tau_{ref} + \ln\left(\frac{\mu}{\mu - 1}\right). \tag{12}$$

Unperturbed heterogeneous neurons fire at constant intervals T_μ, so that the ISI densities $\rho_{LIF}\,(T;\mu, D=0)$ of the heterogeneous neurons are δ-functions. For simplicity we can map the probability distribution expressed in μ to the variable $T := T_\mu$, $P\,(\mu)\,d\mu = \hat{P}(T)dT$, because the function that relates both variables, Eq. (12), is monotonically decreasing. Making use of the fact that the ISI densities of heterogeneous neurons are delta distributed and applying Eqs. (10) and (11) we obtain

$$\rho_{hom}\,(T;\, D_{hom}, \mu_{hom}) \stackrel{!}{=} \frac{\hat{P}(T)T^{-1}}{\int dT'\;(T')^{-1}\,\hat{P}\,(T')}. \tag{13}$$

The r.h.s above is a probability density function (denoted as $Q(T)$ in Fig. 1A), which must be equal to the homogeneous ISI density. Introducing Eq. (12) in the expression above and solving for $P\,(\mu)$ we obtain

$$P\,(\mu) = \left(\tau_{ref} + \ln\frac{\mu}{\mu-1}\right)\frac{\rho_{hom}\left(T = \tau_{ref} + \ln\frac{\mu}{\mu-1}\right)}{\mu\,(\mu-1)\;\langle T\rangle_{hom}}, \tag{14}$$

where $\langle T\rangle_{hom}$ denotes the mean interspike interval of the homogeneous population. This equation prescribes the distribution of mean inputs for a heterogeneous population of deterministic LIF neurons that displays the same population's ISI density as the given homogeneous population (see Fig. 1B and C for an illustrative example). For the heterogeneous population, the input probability density $P\,(\mu)$ is defined only for $\mu > 1$, since neurons that do not fire spontaneously are not included in our

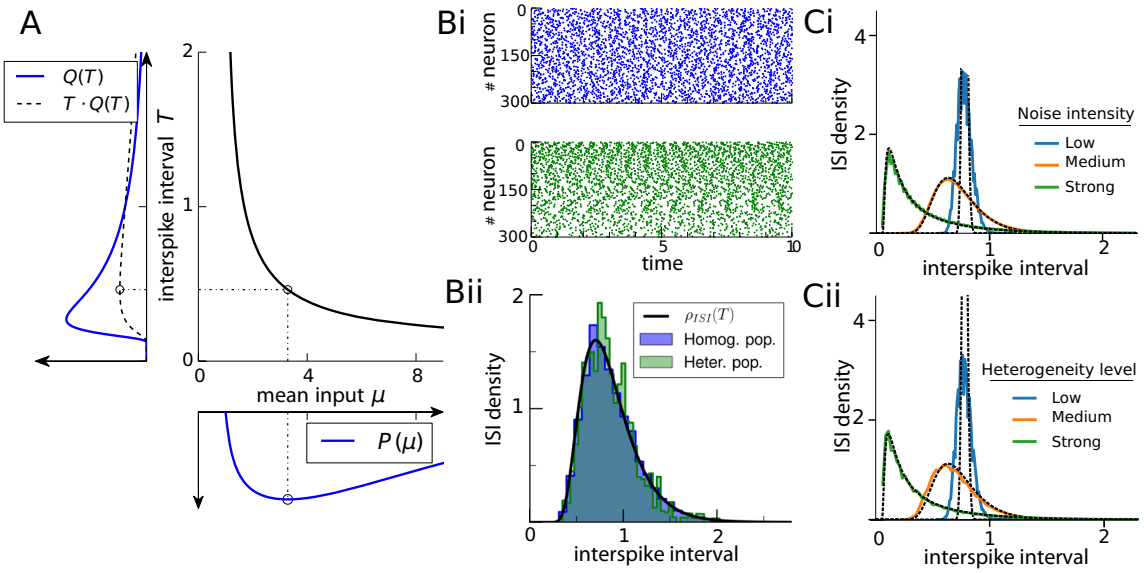

Fig. 1 Homogeneous and heterogeneous populations with same population's ISI density. A Mapping of the probability density of input currents $P\,(\mu)$ of the heterogeneous system to a given homogeneous ISI density $Q(T)$. The ISI probability $Q(T)$ (blue curve, left panel) is multiplied by T and then normalized to unbias the sampling (dashed line). The new density is mapped to the variable μ using Eq. (12) (central panel) to obtain the corresponding $P\,(\mu)$ (bottom panel). **Bi** Rasterplots of the firing activity. Homogeneous neurons (blue) fire stochastically in an unsynchronized manner. Heterogeneous neurons (green) fire at different rates that stay constant throughout the whole recording. For illustrative purposes, the neurons have been sorted according to their spike count. **Bii** ISI densities for the homogeneous (blue histogram) and heterogeneous populations (green histogram) obtained from the data shown in Bi. The solid line shows the analytical ISI density of a homogeneous neuron, Eq. (2). Note the deviations due to finite size effect, which are larger for the heterogeneous population. **C** Comparison of the changes in the ISI histogram when the signal is turned on (colored lines) to the analytical expression when no signal is present (dashed black lines) for three levels of variability for the homogeneous (Ci) and the heterogeneous population (Cii). Parameters $\mu_{hom} = 1.3$, $N = 300$. In panels A and B, $D_{hom} = 0.1$; in panel C, $D_{hom} = 1.8 \cdot 10^{-4}$ (blue), $2.7 \cdot 10^{-2}$(orange) and 1.3 (green); signal standard deviation in C is $\sigma_s = 0.3$

heterogeneous population model. In the following, the mean input current to the homogeneous neurons is held constant unless specified. Consequently, the noise intensity D_{hom} is the only parameter that controls the stochasticity of the homogeneous neurons as well as the level of heterogeneity, so that an increasing value of D_{hom} implies stronger noise and disorder in the homogeneous and heterogeneous systems, respectively.

The criterion links the two types of variability when there is no input signal present. However, in order to reasonably compare the information transmission properties of these two neural ensembles, the ISI densities should still share a high degree of similarity when the input signal is turned on. For low levels of variability, the input signal considerably alters the ISI density (compare blue with dashed black line in Fig. 1C). Nevertheless, the population ISI densities of both systems are modified in a very similar way (compare blue lines in Fig. 1Ci and Cii). For populations with stronger variability, the changes in the ISI density are less pronounced in the two studied systems (cf. orange lines in Fig. 1C), and approach the unperturbed ISI density as the variability is even stronger (green lines, Fig. 1C).

4 Signal transmission in the face of dynamic noise or disorder (heterogeneity)

Information transmission in the homogeneous and heterogeneous systems critically depends on the amount of variability that is present. In line with the classical findings on suprathreshold stochastic resonance (Stocks and Mannella 2001; McDonnell et al. 2007), we qualitatively identified three different behaviors for low, medium and high intensity of the noise/disorder based on two properties of the response function: the variability across neurons in the population (variability in the activity in the vertical lines of the raster-plots in Fig. 2) and the variability across trials upon repetition of the stimulus (difference between colored lines in the output panels of Fig. 2). Trial-to-trial variability comes about because on each trial new realizations of dynamical noise are generated in the homogeneous population and N new values of μ_i are drawn from the distribution $P(\mu)$ for the heterogeneous population. For weak noise or small heterogeneity level the whole population conveys almost the same information as a single neuron (Fig. 2 top), since almost all neurons fire perfectly in synchrony. The repetition

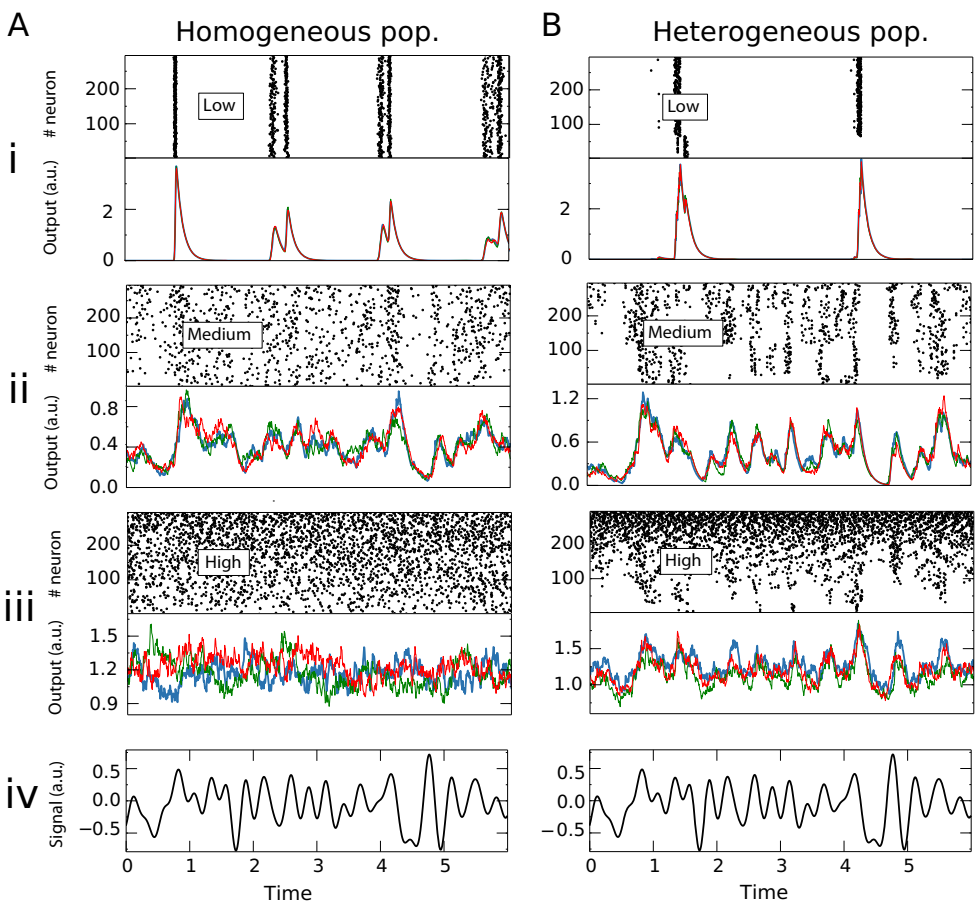

Fig. 2 Effects of noise and disorder on the population firing rate. Population raster plot of one trial and three different trials (colored lines) of the filtered population activity (output function) of the homogeneous (left panel **A**) and heterogeneous (right panel **B**) populations for three different equivalent noise/heterogeneity level intensities ($D_{hom} = 3.4 \cdot 10^{-5}$ (i), $2.7 \cdot 10^{-2}$ (ii) and 6.9 (iii)). Populations are stimulated by the same signal; on every trial, dynamical noise for the homogeneous population and static input currents μ_i for the heterogeneous population are independently generated and drawn from $P(\mu)$, respectively. The initial voltage values of neurons in both populations are initiated at random values (uniformedly distributed between -0.1 and 0.9). An initial time window of $T = 10$ is discarded to avoid transient effects. (iv). In the raster plots, the neurons have been sorted by their spike count. Remaining parameters: $\mu_{hom} = 1.3$, $f_c = 4.0$, $\sigma_s = 0.3$, $N = 300$

of a frozen stimulus also leads to the same population response. For intermediate noise intensities, the variability gives rise to moderately different spike trains of the neurons. Therefore, the population response, which averages over all these different responses, is able to convey more information about the stimulus. The trial-to-trial variability stays low, so that the population response is reliable (Fig. 2, middle). Finally, high intensities of dynamic noise or heterogeneity result in a strong neural variability that overcomes the averaging of the response, so that the system transfers less information about the stimulus (Fig. 2, bottom).

Despite these common properties between dynamic noise or disorder, clear differences can also be observed especially at high variability levels. A wide distribution of the mean input current in the heterogeneous population implies that some neurons hardly emit any spikes while others are firing at very high rates. The almost silent heterogeneous neurons barely convey any information at all, reducing the effective size of the population, and the very active neurons fire constantly, barely influenced by the stimulus, introducing signal-unrelated information in the population's response. Strong dynamic noise influences the response straightaway, by provoking the effective disappearance of the input signal, such that the intrinsic noise sources dominate the output.

In the following, we systematically quantify by means of the coding fraction how the transmission of information in the two scenarios is affected by the stimulus properties (amplitude and cutoff frequency) and by the properties of the population (size and firing regime of single neurons).

4.1 Dependence on stimulus amplitude and cutoff frequency

In Fig. 3 we plot the coding fraction vs the system variability for various values of the stimulus strength. Weak noise or low disorder leads to a low coding fraction value which is very similar in both systems. At intermediate levels of noise or heterogeneity the coding fraction reaches a maximum. Finally, for strong noise or high disorder the transmission efficiency reduces again the coding fraction values. This resonant-like behavior of the encoding efficiency as a function of noise/disorder is observed for a large range of stimulus amplitudes. The amount of noise intensity/heterogeneity required to maximize the coding fraction increases with stimulus strength (Fig. 3i). However, there are differences between noise and heterogeneity with respect to the dependence on the amplitude. A larger input amplitude corresponds systematically to a higher coding fraction value at the optimal (dynamic) noise intensity. This is not the case for very disordered systems, where stronger stimuli do not always yield a larger optimal coding fraction (cf. blue and orange lines, Fig. 3Bi).

The actual value of the coding fraction in nonlinear systems also depends strongly on the properties of the input stimulus, such as the cutoff frequency. In Fig. 3Aii there is a factor two between the maximal coding fraction of the homogeneous population for a low cutoff frequency and a high cutoff frequency stimulus. This suggests that high frequencies are less well encoded in the population activity of the homogeneous system, which is in line with

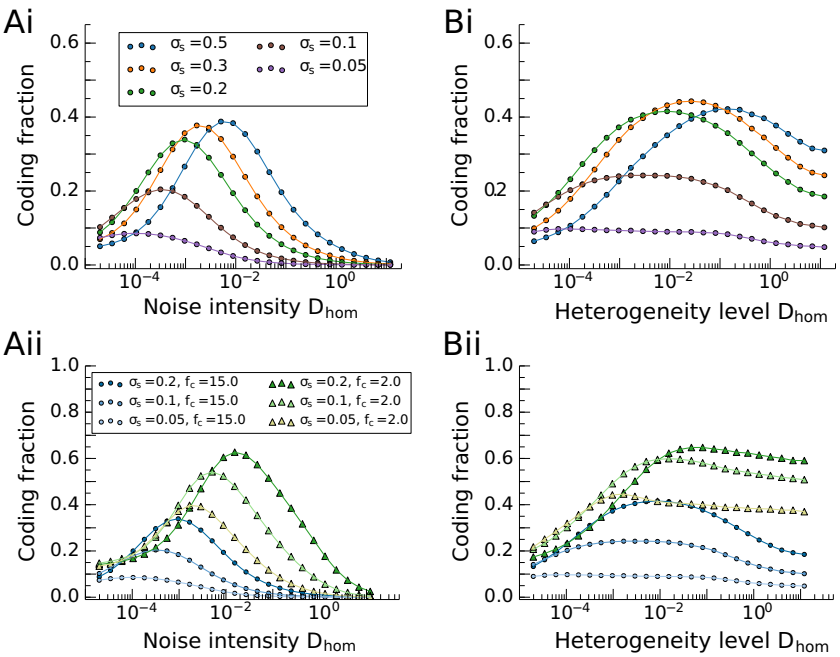

Fig. 3 Dependence of the coding fraction curves on the stimulus parameters. Input-output coding fraction as a function of the noise intensity in the homogeneous system (**A**) and of the level of heterogeneity in the heterogeneous system (**B**). (i) Results for different standard deviations σ_s of the input signal. Cutoff frequency $f_c = 15.0$. (ii) Influence of cutoff frequency: Broad-band stimulus (circles) and low-frequency stimulus (triangles). Parameters: $\mu_{hom} = 1.3$, $N = 300$

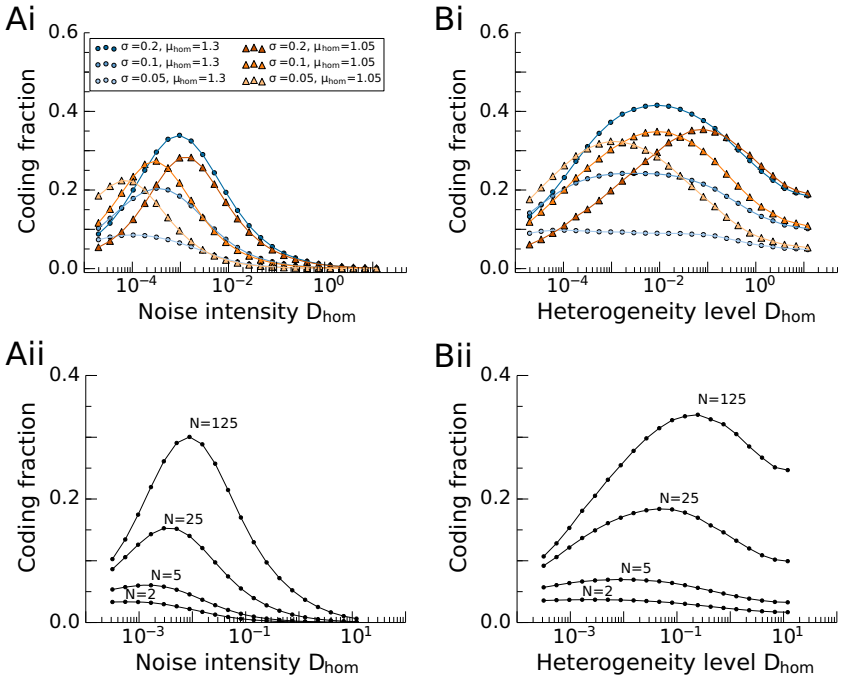

Fig. 4 Dependence of the coding fraction curves on the mean input current and the population size. (i) Comparison of the coding fraction for mean input current far above threshold (circles) and close to threshold (triangles), for **A** homogeneous and **B** heterogeneous systems. (ii) Coding efficiency for different population sizes and an input signal of standard deviation $\sigma_s = 0.5$. Parameters: $\mu_{hom} = 1.3$, $f_c = 15.0$, and in panels Ai and Bi $N = 300$

the finding that LIF neurons act as low-pass filters of information (Vilela and Lindner 2009b; Lindner 2016). In the heterogeneous population, a similar relation in the coding fraction between low- and high-frequency stimuli is observed. However, the coding fraction varies in shape, since the decay after the maximum coding fraction is much steeper for higher cutoff frequencies. This implies that heterogeneity affects more the processing of stimulus components in higher frequency bands.

4.2 Dependence on mean input current and system size

Two opposite effects influence the coding fraction when the mean input current μ_{hom} is varied. On the one hand, for low mean input currents (close to but slightly above threshold) and sufficiently strong stimuli, the negative parts of the signal are able to silence the network temporarily, so that no spikes are emitted in the whole system. For that reason, a lower mean input current reduces the coding fraction in both systems if the amplitude is large enough (Fig. 4i, dark blue above dark brown curves). On the other hand, if the input signal is not that strong, input currents μ_{hom} closer to threshold increase the relative strength of the input stimulus. Consequently, as shown above, weaker stimuli can be more easily conveyed by both populations, increasing the coding fraction (Fig. 4Ai and Bi, lighter brown above light blue curves).

The considered output function, the population activity, can be regarded as an average over the different units of the population. The resonant-like effect in the coding fraction depends on the trial-to-trial variability and variability across the population, so that the size of the system influences the curves (Fig. 4Aii and Bii) in a similar way for both noisy homogeneous and deterministic heterogeneous populations. For the single mean-driven neuron, there is no resonance effect. For groups of neurons, the suprathreshold stochastic resonance effect emerges and becomes more pronounced with increasing population size.

4.3 Comparing and combining both kinds of variability

It is possible to compare the encoding efficiency of noise and disorder by subtracting the coding fraction of the homogeneous system from the heterogeneous one. This difference is plotted as a heatmap (Fig. 5) with axes: the noise intensity/level of heterogeneity D_{hom} (x-axis) and the standard deviation of the stimulus σ_s (y-axis). Note that the map does not indicate how well these two systems perform at encoding the signal but how much better one system performs compared to the other one for given level of noise/heterogeneity and a given signal strength. For a neural population receiving weak stimuli ($\sigma_s < 0.2$, Fig. 5A), heterogeneity is always more beneficial for the information flow than intrinsic noise. With dynamic noise, the time-dependent stimulus competes directly with the noise stimulus in affecting the system's dynamics and this competition makes it more difficult to faithfully encode a weak stimulus. The heterogeneous population can still convey information about these weak stimuli because the mean input current distribution acts in a more indirect way at

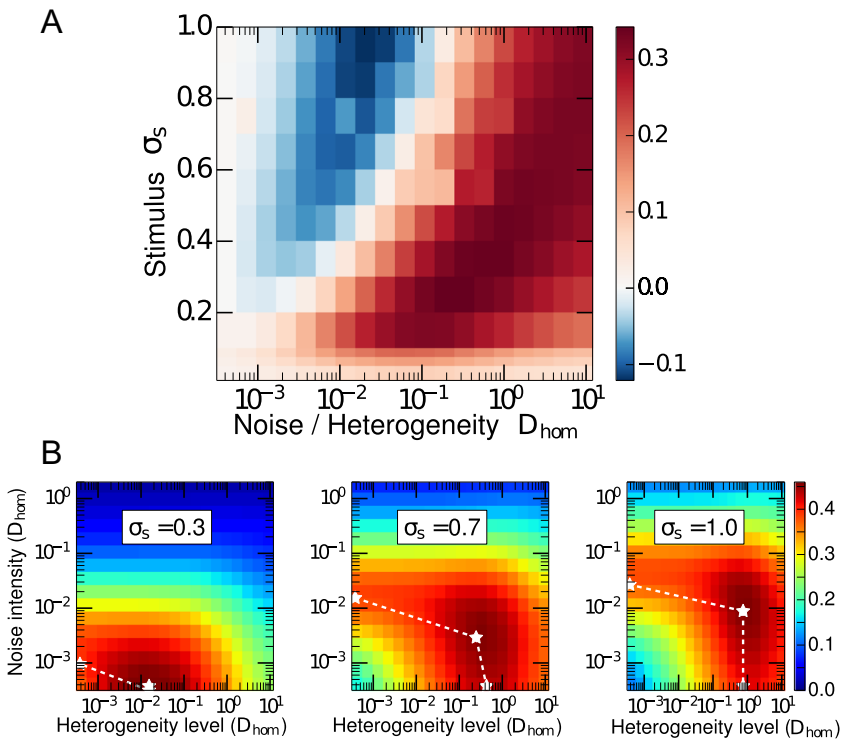

Fig. 5 Comparison of noise and heterogeneity. A Comparison of the coding performance in the presence of either just noise or just disorder. Difference between the coding fraction of the two systems, $\gamma_{het} - \gamma_{hom}$. Blue colors: the homogeneous system encodes better the information (negative sign), red colors: the heterogeneous population encodes better (positive sign). The color intensity denotes the absolute magnitude of this difference. **B** Coding fraction of a neural population combining both noise and heterogeneity. White stars mark the maximum coding fraction for the combination of noise and disorder, just for heterogeneity and just for noise (on x- and y-axis correspondingly). White dashed lines joining the stars are guides to the eye. Parameters: $\mu_{hom} = 1.3$ and $f_c = 15.0$ and $N = 300$

desynchronizing the neurons. As a consequence, very high levels of disorder are less harmful than very strong noise for encoding weak time-dependent signals.

For strong stimuli, dynamic noise is more helpful for encoding than the same amount of disorder (heterogeneity) up to a certain level, and beyond this optimal level, disorder outperforms dynamic noise. Because for stronger signals the heterogeneous system attains its maximum at a larger level of input variability than the homogeneous system with dynamic noise does (see Fig. 3Ai, Bi), the difference between the two curves has to attain first negative and then positive values. Note that in this case the maximum of the coding fraction for the heterogeneous system is still slightly larger than that for the homogeneous system (but attained at larger input variability).

These complementary properties in processing different stimuli suggest that a certain neural population might optimize its levels of dynamic noise or disorder based on the type of stimuli that they encode. Furthermore, most systems exhibit a wide range of rate heterogeneity and are subject to noise sources at the same time. Figure 5B shows three examples of how the presence of both noise and heterogeneity affect the coding performance, for three different signal strengths. Hunsberger et al. (2014) stated that both noise and heterogeneity share similar operating mechanisms; both of them desynchronize the spike trains of the different neurons and linearize the input-output transfer function, so that the effects of those two types of variability do not add up linearly. For that reason, when combining dynamic noise and heterogeneity in a neural population, the optimal combination of dynamic noise and disorder is reached at a lower value of dynamic noise (left and right panels in Fig. 5B) or even at both lower dynamic noise and heterogeneity levels (Fig. 5B, middle panel).

Heterogeneity is not able to affect the signal processing when there is already strong noise in the system (horizontal rows at the top of the heatmaps, Fig. 5B). We can also observe that the optimal combination of noise and heterogeneity requires higher values of D_{hom} for stronger signals, just as it happened when only one form of input variability is present.

4.4 Analytically tractable limit cases

The input-output coding fraction for an arbitrary input signal and neural population cannot in general be expressed in an analytical form. The coding fraction is determined by the coherence function and the stimulus power spectrum. The coherence itself depends on the output power spectrum of the population and the input-output cross-spectrum. Unfortunately, these spectral properties of the homogeneous and heterogeneous populations cannot be calculated analytically for arbitrarily strong inputs. Nevertheless, there are two limit cases in which analytical approximations can be obtained. In one case, given that the stimulus intensity is small compared to the intrinsic noise intensity and assuming that the stimulus is white and Gaussian (i.e. for high cutoff frequencies), the single neuron power spectrum

and cross-spectrum of the homogeneous population can be approximated by linear response theory.

The population's output power spectrum of the homogeneous population is fully determined by the single neuron power spectrum $S_{x_i x_i}$ (same for all neurons i) and cross-spectrum between different neurons $S_{x_i x_j}$ (same for any pair of neurons in the homogeneous population) as

$$S_{xx}(f) = \frac{1}{N}\left(S_{x_i x_i}(f) + (N-1)\, S_{x_i x_j}(f)\right), \tag{15}$$

which is obtained by applying the definition of the power spectrum, Eq. (4), and the output function, Eq. (3).

At the single neuron level, there is no difference in the processing of noise or signal, both inputs are added up. The signal is considered white with the same intensity as the band-limited Gaussian noise, $D_s = \int_0^\infty d\tau\, \langle s(t)s(t+\tau)\rangle = \sigma_s^2/(4f_c)$. The single-neuron power spectrum $S_{x_i x_i}$ is then given by Eq. (5) where the total input intensity D comprises both the noise and signal contributions, $D = D_{hom} + D_s$. Using the definition Eq. (4) and the linear response ansatz, Eq. (6), the cross-spectrum between neurons reads (Ostojic et al. 2009a; Vilela and Lindner 2009b)

$$S_{x_i x_j}(f) = \lim_{T_W\to\infty}\frac{1}{T_W}\langle \chi^*\tilde{s}^* \cdot \chi\tilde{s}\rangle = |\chi(f)|^2\, S_{ss}(f). \tag{16}$$

The cross-spectrum between input, $s(t)$, and population's output, Eq. (3), is the same as the cross-spectrum between input and single neuron spike train for the homogeneous population:

$$\begin{aligned} S_{xs}(f) &= \lim_{T_W\to\infty}\frac{1}{T_W}\langle \tilde{x}^*\tilde{s}\rangle = \frac{1}{N}\sum_{i=1}^{N}\lim_{T_W\to\infty}\frac{1}{T_W}\langle \tilde{x_i}^*\tilde{s}\rangle \\ &= \chi^*(f)\, S_{ss}(f). \end{aligned} \tag{17}$$

Finally, the coherence function can be analytically approximated in terms of the susceptibility, the power spectrum of the stimulus and the spectrum of the single neuron output using Eqs. (15), (16), (17) and the definition of coherence in Eq. (8):

$$C(f) = \frac{N\,|\chi(f)|^2\, S_{ss}(f)}{S_{x_i,x_i}(f) + (N-1)\,|\chi(f)|^2\, S_{ss}(f)}. \tag{18}$$

The coding fraction can be obtained numerically integrating the analytical expression above within the stimulated frequency range. The coherence approximation, however, only works for input signals whose intensity is orders of magnitude smaller than the noise intensity of the system (Fig. 6A, green line), i.e. in the regime in which noise linearizes the signal transfer (Hunsberger et al. 2014). For stronger stimuli or weaker noise, the approximation completely fails at describing the features of the coherence. First of all, the firing rate modulation itself and thus the cross-spectrum between input signal and output spike trains undergoes a nonlinear modification (Brunel and Hakim 1999; Ostojic and Brunel 2011; Voronenko and Lindner 2017). Secondly, the cross-spectrum between neurons, Eq. 16, appearing in the power spectrum of the

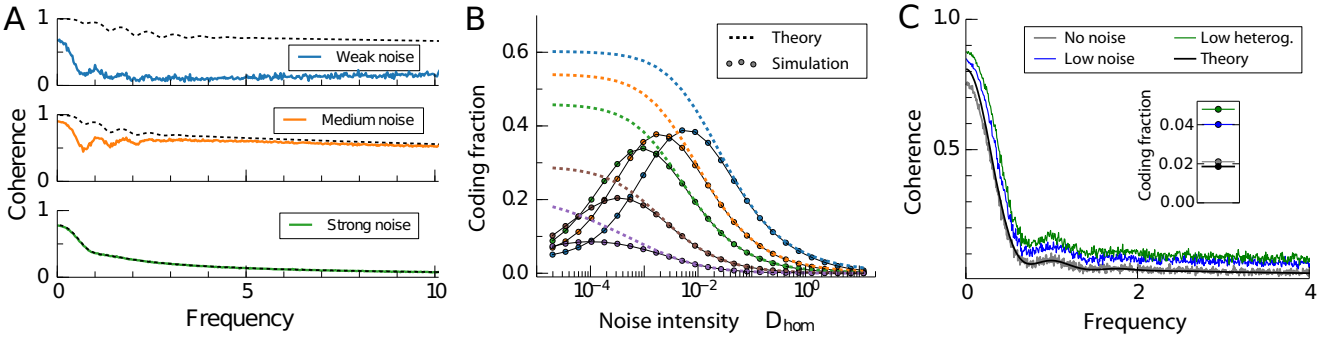

Fig. 6 Approximations of the coherence and coding fraction curves. A Linear response theory approximations (dashed lines) of the spectral coherence, Eq. (18), in comparison to simulation results (solid lines) for the homogeneous population for three different noise intensities. For moderate and low noise intensities, the theoretical curves remain close to each other, although far away from the simulation results. Intrinsic noise intensities $D_{hom} = 1.9\cdot 10^{-4}, 9.5\cdot 10^{-3}$ and $4.6\cdot 10^{-1}$ for weak, medium, and strong noise respectively. Stimulus $\sigma_s = 0.2$, which corresponds to a noise intensity $D_s = 6.6\cdot 10^{-4}$. **B** Coding fraction curves of the homogeneous population: dashed lines have been semi-analytically calculated with Eqs. (18) and (9); dots correspond to the simulation results, color legend as in Fig. 3Ai (thin gray lines serve only as visual guides). **C** Single-neuron approximation for weak noise/disorder: analytical expression of the coherence function (black line) and numerically calculated coherence for a noiseless homogeneous system (gray line) and for the noisy homogeneous and heterogeneous systems (blue and green lines) with very low stochasticity ($D_{hom} = 1.5\cdot 10^{-5}$, $\sigma_s = 0.5$); inset: corresponding coding fraction values. Common parameters in all panels: $\mu_{hom} = 1.3$ and for the numerically simulated data $f_c = 15.0$, $N = 300$

population, is largely underestimated, because the signal synchronizes the neurons more than what linear response theory would predict, leading to an overestimation of the true coherence function (blue and orange in Fig. 6A). As a consequence, this analytical approximation can only describe the decay to zero of the coding fraction curve for very large noise intensities. The emergence of a maximal coding fraction is only explained by the nonlinearity and the population finite-size effect (Fig. 6B).

A second limit case can be analytically calculated for both populations: the case of noise or heterogeneity tending to zero. Having (almost) no noise and no heterogeneity in a population is equivalent to just one neuron, because the spike trains of all neurons in the population become identical if they are driven by exactly the same stimulus (no intrinsic noise, no difference in the mean input). This single-neuron limit case can already be conjectured in Figs. 3 and 4, where the coding fraction curves for a given stimulus seem to tend to the same non-zero value in both populations. In order to calculate this value, it is necessary to compute the output power spectrum and the cross-spectrum. Assuming again that the stimulus is described by a white Gaussian noise process of intensity D_s, the output power spectrum of the single neuron is given by Eq. (5) while for the cross-spectrum one finds (Vilela and Lindner 2009b):

$$S_{xs}(f) = 2D_s \chi(f; D_s, \mu_{hom}). \tag{19}$$

The coherence can be thus calculated analytically (Fig. 6C, black line) and integrated numerically according to Eq. (9) to obtain the coding fraction of a single neuron stimulated with white noise. In Fig. 6C, the analytical expression of the coherence is compared to the homogeneous and heterogeneous systems at low noise/disorder (blue and green lines) and to the simulation of a noiseless homogeneous population (gray line). The small deviation between the analytical expression and the simulation of a noiseless population can be ascribed to the effects of a finite trial length. We note that without intrinsic noise, long transients are required to see the convergence to the same spike train (we recall that the system is started with random initial conditions). This convergence was an important assumption in identifying the system in this limit with the single-neuron case. The single neuron limit case constitutes a lower bound of the coding fraction for low stochasticity levels, but the difference in coding fraction is still considerable even for a small intrinsic noise.

In summary, we can state that the analytically tractable limit cases strongly suggest the existence of optimal values of the coding fraction. Signal transmission becomes worse by increasing the noise intensity to large values (according to the linear-response theory) but is rather small in the limit of vanishing intrinsic noise (according to the single-neuron theory). Unfortunately, the exact optimal value of noise intensity or disorder parameter is difficult to assess analytically. The regime of weak intrinsic noise for a neural population with common time-dependent drive seems to be especially difficult and constitutes a substantial challenge for future theoretical efforts.

5 Summary

Dynamic noise and *heterogeneity* are present in most neural systems. Both can be understood as a stochastic variation, either in the dynamics of the input space or in the parameter space. Here, we compared two populations of uncoupled units: the *homogeneous population*, consisting of identical neurons that receive independent additive noise on top of the stimulus, and the *heterogeneous population*, in which deterministic neurons receive the same stimulus but different constant input currents. We achieved a fair comparison between the different forms of input variability by enforcing the same ISI density for both populations and focussed on the coding fraction as a measure of information transmission for time-dependent stimuli with a high cutoff frequency.

Kind of neural populations considered and the validity of our assumptions We made several assumptions that simplify the mathematical description of the neural populations while still accounting for essential properties of many sensory feed-forward networks. First, we considered only populations of uncoupled neurons receiving a common stimulus. This approximates a common design of many peripheral sensory systems, like for instance the auditory, vestibular, olfactory and electrosensory systems. The assumption of uncoupled neurons allowed us to relate the theory of suprathreshold stochastic resonance (based on parallel units processing a common stimulus) to neural networks with a strong feed-forward component. Obviously, recurrent neural networks of spiking neurons show a wider variety of firing regimes (Abbott and van Vreeswijk 1993; Brunel 2000; Litwin-Kumar and Doiron 2012; Ostojic 2014). How to quantitatively compare the effects of heterogeneity and noise in such networks remains an open question. Even in homogeneous recurrent networks, the noise level is not a simple control parameter anymore because a strong effective stochasticity arises from the nonlinear interaction between many spiking neurons (Abbott and van Vreeswijk 1993; Brunel 2000). The intensity and correlation statistics of this network noise strongly depends on cellular and network parameters (Lerchner et al. 2006; Dummer et al. 2014; Ostojic 2014; Wieland et al. 2015) in ways that are not yet well understood.

Another assumption of the model is that both populations are composed exclusively of units in the supra-threshold (mean-driven) regime. This is certainly not a very good approximation for cortical neurons but it is consistent with experimental observations of high firing rates and low CVs in first-stage sensory populations, e.g. auditory fibers (Fisch et al. 2012) or P-units and ampullary cells in weakly electric fish (Grewe et al. 2017). For comparison of our (non-dimensional) results with experimental data consider the P-units in weakly electric fish (Grewe et al. 2017): assuming a membrane time constant of 5 ms, typical firing rates ($r = 1.25 \rightarrow 250$ Hz) and stimulus cutoff frequencies ($f_c = 2 \rightarrow 400$ Hz) in our model would be similar to the values observed and used for the P-units ($r = 50 - 450$ Hz and $f_c = 150 - 300$ Hz, respectively).

A methodological reason for having purely supra-threshold mean input currents is that the alternative choice would complicate the comparison between the two setups: in the heterogeneous system of deterministic neurons, a subthreshold mean input current to a certain cell would yield a spontaneous rate of exactly zero for this neuron, and such silent cells could not have a counterpart in the homogeneous population of neurons that are subject to unbounded intrinsic noise (here the firing rate is always strictly positive). To summarize, our setup is intended to mimic populations in the sensory periphery with high firing rates and low CV. How to extend the kind of comparison to recurrent networks of irregularly spiking neurons with low firing rates is an interesting yet highly non-trivial problem for future research.

We would like to emphasize that our setup differs substantially from the one considered previously by Stocks and Mannella (2001) and Hunsberger et al. (2014) in the context of suprathreshold stochastic resonance, which used slow stimuli and considered the instantaneous mutual information between the slow stimulus and a low-pass filtered output variable. Remarkably, however, qualitatively, we recover a number of results made in these previous studies. Our numerical simulations of the two systems revealed that finite levels of noise and heterogeneity clearly optimize the information transmission process similar to the results by Stocks and Mannella (2001) and Hunsberger et al. (2014). Also, we showed that the simultaneous combination of these two variability classes can improve the coding properties. Moreover, we analyzed the effect of modifying the input signal intensity, cutoff frequency and mean input current, which significantly affect the coding fraction. Two semi-analytical approximations capture our numerical results in the limit cases of vanishing and large intrinsic noise/heterogeneity, respectively. One is based on linear response theory applied to the homogeneous population, which holds true only for strong intrinsic noise. Therefore it does not reproduce the resonance effect of noise. The second approach sets a lower bound for the coding fraction and coherence function for weak noise intensities or small levels of heterogeneity. In that limit case, the two populations behave in a similar way to a single neuron, whose coding fraction for a given stimulus can be semi-analytically computed. The combination of the two approaches, supported by our simulation results, strongly suggests the existence of an optimal noise level (potentially also several ones). However, the calculation of the exact value (or values) at which the coding fraction is optimized is still an open theoretical problem.

Noise vs heterogeneity The resemblance of dynamic noise and heterogeneity is manifest. Both variabilities can enhance the transmission of information. In populations of spiking neurons, independent dynamic noise desynchronizes the spike trains of the population and linearizes the transfer function of individual neurons (Hunsberger et al. 2014). The results presented in this study nonetheless reveal that neural populations might preferably show a higher level of heterogeneity or noise intensity depending on the stimuli they process. Adding dynamic noise to a population of heterogeneous neurons can improve the maximum possible coding fraction if the stimulus amplitude is large enough (Fig. 5B). This is in contrast to the original findings reported for heterogeneous threshold arrays, where the maximum mutual information obtained by adding dynamic noise was always below the one obtained for an optimal level of heterogeneity (Stocks 2000).

In a recent study, Grewe et al. (2017) found that two cell populations in the electrosensory system of weakly electric fish show differences both in the intrinsic noise level (as becomes apparent in the single neuron's coefficient of variation of the interspike interval) and in the level of heterogeneity (as becomes apparent in the population distribution of firing rates): while the so-called P-units are both variable with respect to firing rates and with respect to intrinsic noise level, the ampullary cells have very little noise and small heterogeneity (cf. in particular, Fig. 1D and E in Grewe et al. (2017)). Hence, in this case it is a combination of dynamic noise and population heterogeneity that seems to be most beneficial for signal transmission. How to relate the levels of intrinsic noise and heterogeneity to the typical bandwidth and stimulus intensities of natural electric stimuli is an interesting open problem.

Suprathreshold stochastic resonance in heterogeneous systems Suprathreshold stochastic resonance (SSR) refers to the effects of dynamic noise in certain nonlinear parallel multi-unit systems. It describes how a finite level of independent noise in the parallel units optimizes information transmission and has been observed in many different systems. Many properties of SSR have also been found

in heterogeneous systems. For instance, heterogeneity by itself, without any other intrinsic noise sources, enhances the amount of information transferred by parallel feed-forward units (Stocks 2000). The magnitude of the "resonance" depends drastically on the number of neurons in the population. The advantageous effects of heterogeneity apply to both weak and strong stimuli, even though at different scales.

In conclusion, heterogeneity renders similarly profitable effects for neural populations as dynamic noise. We can then affirm that suprathreshold stochastic resonance –understood in the broadest sense of the term– is observed as well in heterogeneous populations of sensory model neurons. Therefore, the same reasons that suggest a decisive role for dynamic noise in sensory systems apply to the presence of heterogeneity.

Compliance with Ethical Standards

Conflict of interests The authors declare that they have no conflict of interest.

Code sharing Source code for the numerical and analytical approximations of this article can be found at: https://github.com/emebeiran/noise_vs_heterog.

References

Abbott, L., & van Vreeswijk, C. (1993). Asynchronous states in networks of pulse-coupled oscillators. *Physical Review E*, *48*, 1483.

Alijani, A., & Richardson, M.J.E. (2011). Rate response of neurons subject to fast or frozen noise: from stochastic and homogeneous to deterministic and heterogeneous populations. *Physical Review E*, *84*, 011,919–1.

Ashida, G., & Kubo, M. (2010). Suprathreshold stochastic resonance induced by ion channel fluctuation. *Physica D*, *239*, 237.

Benzi, R., Sutera, A., Vulpiani, A. (1981). The mechanism of stochastic resonance. *Journal of Physics A*, *14*, L453.

Brunel, N. (2000). Dynamics of sparsely connected networks of excitatory and inhibitory spiking neurons. *Journal of Computational Neuroscience*, *8*, 183.

Brunel, N., & Hakim, V. (1999). Fast global oscillations in networks of integrate-and-fire neurons with low firing rates. *Neural Computation*, *11*, 1621.

Brunel, N., Chance, F.S., Fourcaud, N., Abbott, L.F. (2001). Effects of synaptic noise and filtering on the frequency response of spiking neurons. *Physical Review Letters*, *86*, 2186.

Chacron, M.J., Longtin, A., Maler, L. (2003). The effects of spontaneous activity, background noise, and the stimulus ensemble on information transfer in neurons. *Network: Computation in Neural Systems*, *14*, 803.

Chance, F.S., Abbott, L.F., Reyes, A.D. (2002). Gain modulation from background synaptic input. *Neuron*, *35*, 773.

Chelaru, M., & Dragoi, V. (2008). Efficient coding in heterogeneous neuronal populations. *Proceedings of the National Academy of Sciences of the United States of America*, *105*, 16,344.

Cox, D.R., & Lewis, P.A.W. (1966). *The statistical analysis of series of events*. London: Chapman and Hall.

Darling, D.A., & Siegert, A.J.F. (1953). The 1st passage problem for a continuous markov process. *Annals of Mathematical Statistics*, *24*, 624.

Das, A., Stocks, N.G., Hines, E.L. (2009). Enhanced coding for exponentially distributed signals using suprathreshold stochastic resonance. *Communications in Nonlinear Science*, *14*, 223.

Dummer, B., Wieland, S., Lindner, B. (2014). Self-consistent determination of the spike-train power spectrum in a neural network with sparse connectivity. *Frontiers in Computational Neuroscience*, *8*, 104.

Durrant, S., Kang, Y., Stocks, N., Feng, J. (2011). Suprathreshold stochastic resonance in neural processing tuned by correlation. *Physical Review E*, *84*, 011,923.

Fisch, K., Schwalger, T., Lindner, B., Herz, A., Benda, J. (2012). Channel noise from both slow adaptation currents and fast currents is required to explain spike-response variability in a sensory neuron. *Journal of Neuroscience*, *32*, 17,332.

Fox, R.F. (1997). Stochastic versions of the hodgkin-huxley equations. *Biophysical Journal*, *72*, 2068.

Gabbiani, F., Metzner, W., Wessel, R., Koch, C. (1996). From stimulus encoding to feature extraction in weakly electric fish. *Nature*, *384*, 564.

Gammaitoni, L., Hänggi, P., Jung, P., Marchesoni, F. (1998). Stochastic resonance. *Reviews of Modern Physics*, *70*, 223.

Golomb, D., & Rinzel, J. (1993). Dynamics of globally coupled inhibitory neurons with heterogeneity. *Physical Review E*, *48*, 4810.

Grewe, J., Kruscha, A., Lindner, B., Benda, J. (2017). Synchronous spikes are necessary but not sufficient for a synchrony code. *Proceedings of the National Academy of Sciences of the United States of America*, *114*, E1977.

Gussin, D., Benda, J., Maler, L. (2007). Limits of linear rate coding of dynamic stimuli by electroreceptor afferents. *Journal of Neurophysiology*, *97*, 2917.

Harrison, P.M., Badel, L., Wall, M.J., Richardson, M.J.E. (2015). Experimentally verified parameter sets for modelling heterogeneous neocortical pyramidal-cell populations. *PLoS Computational Biology*, *11*, 8.

Hoch, T., Wenning, G., Obermayer, K. (2003). Optimal noise-aided signal transmission through populations of neurons. *Physical Review E*, *68*, 011,911–1.

Homstron, L., Eeuwes, L., Roberts, P., Porfors, C. (2010). Efficient encoding of vocalizations in the auditory midbrain. *Journal of Neuroscience*, *30*, 802.

Hromádka, T., DeWeese, M., Zador, A. (2008). Sparse representation of sounds in the unanesthetized auditory cortex. *PLoS Biology*, *6*, 0124.

Hunsberger, E., Scott, M., Eliasmith, C. (2014). The competing benefits of noise and heterogeneity in neural coding. *Neural Computation*, *26*, 1600.

Lerchner, A., Sterner, G., Hertz, J., Ahmadi, M. (2006). Mean field theory for a balanced hypercolumn model of orientation selectivity in primary visual cortex. *Network: Computation in Neural Systems*, *17*, 131.

Lindner, B. (2016). Mechanisms of information filtering in neural systems. *IEEE Transactions on Molecular Biological and Multiscale Communications*, *2*, 5.

Lindner, B., & Schimansky-Geier, L. (2001). Transmission of noise coded versus additive signals through a neuronal ensemble. *Physical Review Letters*, *86*, 2934.

Lindner, B., Schimansky-Geier, L., Longtin, A. (2002). Maximizing spike train coherence or incoherence in the leaky integrate-and-fire model. *Physical Review E*, *66*, 031,916.

Litwin-Kumar, A., & Doiron, B. (2012). Slow dynamics and high variability in balanced cortical networks with clustered connections. *Nature Neuroscience*, *15*, 1498.

Longtin, A. (1993). Stochastic resonance in neuron models. *Journal of Statistical Physics*, *70*, 309.

Maler, L. (2009). Receptive field organization across multiple electrosensory maps. *Journal of Comparative Neurology*, *516*, 376.

Marsat, G., & Maler, L. (2010). Neural heterogeneity and efficient population codes for communication signals. *Journal of Neurophysiology*, *104*, 2543.

McDonnell, M.D., & Ward, L.M. (2011). The benefits of noise in neural systems: bridging theory and experiment. *Nature Reviews Neuroscience*, *12*, 415.

McDonnell, M.D., Stocks, N.G., Abbott, D. (2007). Optimal stimulus and noise distributions for information transmission via suprathreshold stochastic resonance. *Physical Review E*, *75*, 061,105.

Mejias, J.F., & Longtin, A. (2012). Optimal heterogeneity for coding in spiking neural networks. *Physical Review Letters*, *108*, 228,102.

Mejias, J., & Longtin, A. (2014). Differential effects of excitatory and inhibitory heterogeneity on the gain and asynchronous state of sparse cortical networks. *Frontiers in Computational Neuroscience* 8.

Metzen, M.G., & Chacron, M.J. (2015). Neural heterogeneities determine response characteristics to second-, but not first-order stimulus features. *Journal of Neuroscience*, *35*, 3124.

Nicolis, C. (1982). Stochastic aspects of climatic transitions - response to a periodic forcing. *Tellus*, *34*, 1.

Nikitin, A., Khovanov, I.A., Morse, R.P., Stocks, N.G. (2010). Enhanced information transmission with signal dependent noise in an array of lif neurons. *European Physical Journal Special Topics*, *187*, 205.

O'Connor, D., Peron, S., Huber, D., Svoboda, K. (2010). Neural activity in barrel cortex underlying vibrissa-based object localization in mice. *Neuron*, *67*, 1048.

Olmi, S., Livi, R., Politi, A., Torcini, A. (2010). Collective oscillations in disordered neural networks. *Physical Review E*, *81*, 046,119.

Osborne, L.C., Palmer, S.E., Lisberger, S.G., Bialek, W. (2008). The neural basis for combinatorial coding in a cortical population response. *Journal of Neuroscience*, *28*, 13,522.

Ostojic, S. (2014). Two types of asynchronous activity in networks of excitatory and inhibitory spiking neurons. *Nature Neuroscience*, *17*, 594.

Ostojic, S., & Brunel, N. (2011). From spiking neuron models to linear-nonlinear models. *PLoS Computational Biology*, *7*, e1001,056.

Ostojic, S., Brunel, N., Hakim, V. (2009a). How connectivity, background activity, and synaptic properties shape the cross-correlation between spike trains. *Journal of Neuroscience*, *29*, 10,234.

Ostojic, S., Brunel, N., Hakim, V. (2009b). Synchronization properties of networks of electrically coupled neurons in the presence of noise and heterogeneities. *Journal of Computational Neuroscience*, *26*, 369.

Padmanabhan, K., & Urban, N. (2010). Intrinsic biophysical diversity decorrelates neuronal firing while increasing information content. *Nature Neuroscience*, *13*, 1276.

Sadeghi, S.G., Chacron, M.J., Taylor, M.C., Cullen, K.E. (2007). Neural variability, detection thresholds, and information transmission in the vestibular system. *Journal of Neuroscience*, *27*(4), 771.

Sceniak, M.P., & Sabo, S.L. (2010). Modulation of firing rate by background synaptic noise statistics in rat visual cortical neurons. *Journal of Neurophysiology*, *104*, 2792.

Schmid, G., Goychuk, I., Hänggi, P. (2004). Effect of channel block on the spiking activity of excitable membranes in a stochastic Hodgkin-Huxley model. *Physical Biology*, *1*, 61.

Shadlen, M., & Newsome, W. (1994). Noise, neural codes and cortical organization. *Current Opinion in Neurobiology*, *4*, 569.

Shafi, M., Zhou, Y., Quintana, J., Chow, C., Fuster, J., Bodner, M. (2007). Variability in neuronal activity in primate cortex during working memory tasks. *Neuroscience*, *146*, 1082.

Shamir, M., & Sompolinsky, H. (2006). Implications of neuronal diversity on population coding. *Neural Computation*, *18*(8), 1951.

Steinmetz, P.N., Manwani, A., Koch, C., London, M., Segev, I. (2000). Subthreshold voltage noise due to channel fluctuations in active neuronal membranes. *Journal of Computational Neuroscience*, *9*, 133.

Stocks, N.G. (2000). Suprathreshold stochastic resonance in multilevel threshold systems. *Physical Review Letters*, *84*, 2310.

Stocks, N.G., & Mannella, R. (2001). Generic noise-enhanced coding in neuronal arrays. *Physical Review E*, *64*, 030,902.

Strong, S.P., Koberle, R., van Steveninck, R.R.D., Bialek, W. (1998). Entropy and information in neural spike trains. *Physical Review Letters*, *80*, 197.

Tripathy, S.J., Padmanabhan, K., Gerkin, R.C., Urban, N.N. (2013). Intermediate intrinsic diversity enhances neural population coding. *Proceedings of the National Academy of Sciences of the United States of America*, *110*, 8248.

Vilela, R.D., & Lindner, B. (2009a). Are the input parameters of white-noise-driven integrate & fire neurons uniquely determined by rate and CV? *Journal of Theoretical Biology*, *257*, 90.

Vilela, R.D., & Lindner, B. (2009b). A comparative study of three different integrate-and-fire neurons: spontaneous activity, dynamical response, and stimulus-induced correlation. *Physical Review E*, *80*, 031,909.

Voronenko, S., & Lindner, B. (2017). Nonlinear response of noisy neurons. *New Journal of Physics*, *19*, 033,038.

van Vreeswijk, C., & Sompolinsky, H. (1996). Chaos in neuronal networks with balanced excitatory and inhibitory activity. *Science*, *274*, 1724.

Wessel, R., Koch, C., Gabbiani, F. (1996). Coding of time varying elcetric field amplitude modulations in a wave-type electric fish. *Journal of Neurophysiology*, *75*, 2280.

Wieland, S., Bernardi, D., Schwalger, T., Lindner, B. (2015). Slow fluctuations in recurrent networks of spiking neurons. *Physical Review E*, *92*, 040,901(R).

Wiesenfeld, K., & Moss, F. (1995). Stochastic resonance and the benefits of noise: from ice ages to crayfish and SQUIDS. *Nature*, *373*, 33.

Wolfart, J., Debay, D., Masson, G.L., Destexhe, A., Bal, T. (2005). Synaptic background activity controls spike transfer from thalamus to cortex. *Nature Neuroscience*, *8*, 1760.